# Reducing Uncertainty in Chemistry Climate Model Predictions of Stratospheric Ozone

A. R. Douglass[1], S. E. Strahan[2], L. D. Oman[1], R. S. Stolarski[3]

[1]NASA Goddard Space Flight Center, Greenbelt MD, USA

[2] University Space Research Association, Columbia, MD, USA

[3]Johns Hopkins University, Baltimore, MD, USA

**Abstract**

Chemistry climate models (CCMs) are used to predict the future evolution of stratospheric ozone as ozone-depleting substances decrease and greenhouse gases increase, cooling the stratosphere. CCM predictions exhibit many common features, but also a broad range of values for quantities such as year of ozone-return-to-1980 and global ozone level at the end of the 21st century. Multiple linear regression is applied to each of 14 CCMs to separate ozone response to chlorine change from that due to climate change. We show that the sensitivity of lower atmosphere ozone to chlorine change $\Delta O_3/\Delta Cl_y$ is a near linear function of partitioning of total inorganic chlorine ($Cl_y$) into its reservoirs; both Cly and its partitioning are controlled by lower atmospheric transport. CCMs with realistic transport agree with observations for chlorine reservoirs and produce similar ozone responses to chlorine change. After 2035 differences in $\Delta O_3/\Delta Cl_y$ contribute little to the spread in CCM results as the anthropogenic contribution to $Cl_y$ becomes unimportant. Differences among upper stratospheric ozone increases due to temperature decreases are explained by differences in ozone sensitivity to temperature change $\Delta O_3/\Delta T$ due to different contributions from various ozone loss processes, each with their own temperature dependence. In the lower atmosphere, tropical ozone decreases caused by a predicted speed-up in the Brewer-Dobson circulation may or may not be balanced by middle and high latitude increases, contributing most to the spread in late 21st century predictions.

## 1. Introduction

If anthropogenic ozone depleting substances (ODSs) were the only change in atmospheric composition, ozone ($O_3$) and stratospheric chlorine would be expected to return to unperturbed levels as ODSs were removed from the atmosphere. Other concurrent changes in composition complicate the picture, and the anticipated increases in greenhouses gases leading to stratospheric cooling and circulation changes are also expected to impact the future global ozone distribution. Stratospheric cooling causes ozone to increase by slowing temperature dependent ozone loss processes. All chemistry climate models (CCMs) predict a speed-up in the Brewer Dobson circulation, leading to a decrease in stratospheric tropical ozone column and increased ozone in middle and high latitudes, depending on the structure of the circulation change [*Austin and Wilson*, 2006; *Shepherd,* 2008; *Waugh et al*., 2009]. In spite of commonalities in simulated ozone evolution as noted by *Oman et al.* [2010], there are significant differences in the predictions that are the subject of this work.

*Eyring et al.* [2005] describe the on-going community effort, sponsored by Stratospheric Processes and Their Role in Climate (SPARC), to evaluate CCMs (CCMVal). The CCMVal project used diagnostics developed from observations to evaluate dynamical, chemical, and radiative processes in CCMs. The CCMs, their simulations, and the results of the evaluations are described in the CCMVal report [*SPARC CCMVal*, 2010, hereafter referred to as *CCMVal2010*]. These simulations were also contributed to the World Meteorological Organization *Scientific Assessment of Ozone Depletion: 2010* [*WMO,* 2011*; hereafter referred to as WMO2011*]. Although CCMVal used observations to show

55 that chemical and transport processes were not well-represented by the CCMs in all
56 cases, this information was not used to discriminate among CCMs. Predictions of 21st
57 century ozone used in WMO2011 were obtained using a time series additive model
58 (TSAM) method described in Chapter 9 of *CCMVal2010* and *Scinocca et al*. [2010] to
59 produce multi-model trends (MMT). The use of such methods to combine results of
60 simulations is widespread in science and economics, and is a better predictor than
61 individual models when the models are independent and unbiased. The CCMs
62 participating in CCMVal and WMO2011 are not completely independent as they share
63 common elements such as the advection scheme or core general circulation model.
64 Perhaps more important, the *CCMVAL2010* evaluation reveals deficiencies for some
65 CCMs such as non-conservation of mass, missing chemical reactions, or poor
66 representation of various processes that result in poor comparisons of constituent
67 distributions with observations. When simulations include known and identified
68 deficiencies, the MMT becomes less credible as the best predictor.
69
70 *Waugh and Eyring* [2008] compared a prediction for total column ozone (TCO) obtained
71 using performance metrics to weight the contributions from various CCMs with an
72 unweighted multi-model mean (MMM), and found only small differences between these
73 weighted and unweighted predictions. Their analysis also revealed some issues with the
74 strategy of weighting contributions to obtain a better prediction, noting that the
75 diagnostics were not independent of each other. In addition, performance on a particular
76 diagnostic of the present atmosphere might or might not be related to the ozone response
77 to composition change.

78 Recent studies have taken a different approach to the use of diagnostics of chemistry and
79 transport diagnostics to explain differences among simulations. *Strahan et al*. [2011] used
80 an expanded set of transport diagnostics for the lower stratosphere to show that four
81 CCMs with the most realistic representation of transport also produced a much narrower
82 range of predicted TCO return-to-1980 dates than the suite of CCMs that contributed
83 simulations to *CCMVAL2010* and *WMO2011*. These same four CCMs also had no
84 significant errors or omissions in their chemical mechanism. *Douglass et al*. [2012]
85 examined the upper stratospheric ozone response to chlorine and temperature. The
86 reaction $O + O_3 \rightarrow 2\ O_2$ and catalytic loss cycles involving chlorine, nitrogen and
87 hydrogen radicals that have the same net effect control upper stratospheric ozone. The
88 temperature dependence of the loss processes varies; $O + O_3$ is most temperature
89 dependent and the chlorine catalytic cycle is least. *Douglass et al*. [2012] showed that
90 the CCMs produce a wide, often unrealistic, range of upper atmospheric temperatures for
91 the present atmosphere. Together that range and differences in constituents such as
92 reactive nitrogen account for differences in the relative importance of the catalytic loss
93 cycles. All of the CCMs predict increases in upper stratospheric ozone as anthropogenic
94 chlorine and temperatures decrease in the 21$^{st}$ century. However, there are differences in
95 the magnitude of increases predicted by the CCMs that become larger as anthropogenic
96 chlorine decreases even though their predicted temperature decreases are similar because
97 the ozone sensitivity to temperature change varies among CCMs. Neither of these studies
98 elucidates the link between transport and lower stratospheric chemistry implied by the
99 *Strahan et al.* [2011] result.
100

101 This paper demonstrates that many of the differences in the predicted evolution of
102 stratospheric ozone can be interpreted and understood using a subset of CCMVal
103 diagnostics and concepts that describe interactions among photochemical, transport and
104 radiative processes that control stratospheric ozone. We apply multiple linear regression
105 (MLR) to the future simulations that were used in the CCMVal exercise and *WMO2011*
106 in order to separate contributions of chlorine change from other factors that contribute to
107 future ozone evolution. MLR has been successfully applied to observational data sets
108 and CCM output to quantify the ozone response to chlorine by accounting for other
109 factors known to affect ozone levels such as volcanic injection of stratospheric aerosols,
110 solar cycle variability and the quasi-biennial oscillation [*Stolarski et al.,* 1991; *Stolarski*
111 *et al.,* 2006]. This approach was also applied to future simulations to separate the ozone
112 response to chlorine change from that due to other changes in composition and climate
113 [*Stolarski et al.,* 2009; *Oman et al.,* 2010]. The results of this separation will then be
114 examined with two goals. The first is to explain the narrower range of values for the
115 predicted year of ozone return to 1980 that is obtained from CCMs with the most realistic
116 performance on transport diagnostics as detailed by *Strahan et al.* [2011]. This part of
117 the analysis focuses on the simulated ozone responses to changes in ODSs. The second
118 goal is to explain the differences in the ozone response to the ongoing changes in
119 greenhouse gases (excluding ODSs) that lead to changes in stratospheric circulation and
120 temperature. These differences in response cause the future simulations to diverge from
121 one another in the middle to late 21$^{st}$ century.
122

123 The simulations and the CCMs that produce them are briefly described in section 2.
124 Section 2 also describes datasets that contribute to interpretation of the simulated ozone
125 evolution. The analysis strategy and results are presented in section 3. Section 4
126 describes relationships between the sensitivity of simulated ozone to chlorine change and
127 the simulation of the present atmosphere. Section 5 considers ozone after 2035 as the
128 anthropogenic contribution to chlorine levels decreases and the ozone response to climate
129 change becomes dominant. Results and their implications are summarized in section 6.
130

131 **2. Chemistry Climate Models, Simulations and Data**

132 *2.1 CCMVal Models and Simulations*

133 *Morgenstern et al.* [2010] and *Oman et al*. [2010] present a detailed overview of the
134 models, inputs, and scenarios used in the CCMVal-2 exercise. These models contributed
135 simulations that are evaluated in the *CCMVAL2010* and used in *WMO2011* Chapter 2
136 (Stratospheric Ozone and Surface Ultraviolet Radiation [*Douglass and Fioletov et al.*,
137 2011]) and Chapter 3 (Future Ozone and Its Impact on Surface UV [*Bekki and Bodeker et*
138 *al.*, 2011]. Eighteen groups contributed simulations to CCMVal-2, but for this analysis
139 we include only the fourteen models that contributed a future scenario simulation and
140 whose vertical domain includes the upper stratosphere. These models are listed in Table
141 1. The future scenario (referred to as REF-B2) uses the A1B greenhouse gas scenario
142 from the Intergovernmental Panel on Climate Change (IPCC) [2000] and the revised A1
143 halogen scenario from *WMO* [2007] and *CCMVal2010*. Most models have simulations
144 that cover 1960 – 2099 with 10-year model spin-up prior to 1960. The Unified

145 Model/United Kingdom Chemistry Aerosol Community Model – Met Office
146 (UMUKCA-METO) future simulation ends in 2083.
147
148 2.2 *Observations*
149 We use observations to show how the simulated distributions of reservoir gases such as
150 hydrogen chloride (HCl) and chlorine nitrate ($ClONO_2$) depend on realistic lower
151 stratospheric transport in order to establish context for discussion. We otherwise do not
152 repeat the comprehensive evaluation of photochemistry in Chapter 6 of the *CCMVal2010*
153 report, or identify 'best' simulations that agree with one or more sets of observations.
154
155 *Network for the Detection of Atmospheric Composition Change*
156 A primary goal of the Network for the Detection of Atmospheric Composition Change
157 (NDAAC) is to obtain consistent, standardized, long-term measurements of atmospheric
158 trace gases at a set of globally distributed research stations to detect trends in atmospheric
159 composition. Here we consider timeseries of the total column abundances of HCl and
160 $ClONO_2$ obtained using Fourier Transform Infrared Spectrometers (FTIR) from eight of
161 the long-term measurement sites listed in Table 2. These sites were selected from the 18
162 FTIR locations listed in the measurements and analysis subdirectory to encompass a
163 broad latitude range with temporal records of nine years or longer. *Rinsland et al.* [2003]
164 discuss such measurements in detail, and show that the build-up and leveling off of the
165 sum of HCl and $ClONO_2$ columns from six of these sites and others not included here is
166 consistent with timeseries for surface source gases and with upper stratospheric HCl as
167 measured by the Halogen Occultation Instrument on the Upper Atmosphere Research

168 Satellite, confirming the effectiveness of the Montreal Protocol and its amendments in
169 reducing the anthropogenic contribution to atmospheric chlorine. Details about the
170 measurements are provided by *Rinsland et al.* [2003] and references therein, and can also
171 be obtained from the NDAAC website http://www.ndacc.org/.
172
173 *SciSat Atmospheric Chemistry Experiment*
174 The Atmospheric Chemistry Experiment (ACE) on the Canadian satellite SCI-SAT-1 is a
175 Fourier Transform Spectrometer (FTS). ACE-FTS is a solar occultation instrument that
176 obtains high resolution spectra (0.02 $cm^{-1}$) between 750–4400 $cm^{-1}$ [*Bernath et al.*, 2005].
177 ACE-FTS makes daily measurements in each of two latitudes bands for sunrise and
178 sunset. Vertical profiles are retrieved for up to 15 sunrises and 15 sunsets per day. Of
179 the many species obtained by ACE-FTS, here we use V3 $ClONO_2$ and HCl profiles,
180 focusing on middle latitudes between 50 and 10 hPa.
181
182 **3. MLR Analyses of CCM Ozone Columns**
183 *3.1 Total column ozone time series in CCMs*
184 Figure 1 shows the evolution of differences from 1980 for the 60°S-60°N and 90°S-90°N
185 averages of total column ozone (TCO) simulated by the CCMVal models. The 1980
186 mean is approximated by a five-year average of annual means (1978-1982) to reduce the
187 importance of year-to-year variations. The range of differences among simulations in
188 2100 (~10 DU) is substantially smaller than the range in 2000 (~15 DU) when the
189 stratospheric chlorine was near its peak value. However, the simulated range of ozone
190 loss due to chlorine change is unrealistically large compared with the estimates of ozone

depletion obtained from observations. *WMO2010* reported 60°S-60°N column ozone levels to be 3.5% (~10 DU) less than 1980. The range of simulated increases in global column ozone in 2100 relative to 1980 is comparable to the observed depletion due to anthropogenic chlorine and thus indicates significant uncertainty.

In each panel of Figure 1 the four blue traces identify the simulations from the CCMs that have the most realistic transport based on the expanded version of the tracer diagnostics used in Chapter 5 of *CCMVal2010* as reported by *Strahan et al.* [2011]. The black dashed vertical lines indicate the earliest and latest years for return-to-1980; the blue dashed vertical lines show the narrower range of return years for the CCMs with realistic transport. These ranges are nearly the same for the 60°S – 60°N and 90°S – 90°N averages. The differences from the 1980 mean are more negative around 2000 and more positive beginning ~2050 for the global average compared with the 60°S – 60°N average. The contribution from springtime lower stratosphere polar ozone loss that is included in the global average explains the more negative difference in 2000. Acceleration of the Brewer Dobson Circulation (BDC), predicted by all CCMs [*Butchart et al.,* 2006; *Butchart et al.,* 2010] causes a tropical ozone decrease that is countered by middle and high latitude ozone increases [*Li et al*., 2009]. The high latitude average includes more of the lower stratosphere middle and high latitude ozone increase, explaining the more positive differences from 1980 after 2050 for the 90°S – 90°N averages. Because the differences among the simulations are similar for the both spatial averages, further

213 discussion considers only the 60°S – 60°N that was discussed by *Strahan et al.* [2011]
214 and is commonly considered in the WMO assessments.
215
216 Figure 1 shows that the differences in CCM responses to increasing chlorine vary by ~15
217 DU over a 20-yr period in spite of using identical chlorine source gas boundary
218 conditions. This suggests that the amount and distribution of stratospheric inorganic
219 chlorine ($Cl_y$) in the CCMs varies, resulting in differences in the ozone response to the
220 specified chlorine change.
221
222 In order to quantify and explain such differences in the ozone sensitivity to changes in
223 chlorine and climate, our strategy is to analyze the output from each CCM using multiple
224 linear regression (MLR). This method, which has been applied to observed and
225 simulated timeseries [*Stolarski et al.,* 1991; *Stolarski et al.,* 2009] capitalizes on the
226 length of the simulated time series to separate the contributions of chlorine change and
227 climate change (i.e., circulation and temperature) to ozone evolution. For each CCM the
228 timeseries used in the MLR begins in 1960 and extends to 2083 for the shortest
229 simulation and to within one or two years of 2100 for the others.
230
231 We explored several options for explanatory variables in the MLR. The chlorine change
232 is always represented by equivalent effective stratospheric chlorine (EESC) [*Newman et*
233 *al.,* 2007]. Circulation or climate-related changes are represented by timeseries of
234 monthly mean vertical velocities at 70 hPa averaged for 20°S – 20°N or the normalized
235 timeseries of lower tropical stratosphere gradients in long-lived tracers such as $N_2O$ or

236 $CFCl_3$. In practice, any of these choices is equivalent to a combination of EESC, a linear
237 trend and the time dependence of the change in upwelling (for the few cases where this
238 change is not linear). All options produce similar values for the ozone sensitivities to
239 chlorine change and climate change (including both changes in temperature and
240 circulation) within each CCM. Examples are shown in Figure 2. In each panel, the
241 crosses are the annual average ozone between 60°S and 60°N from a particular CCM.
242 The black solid line is the fit to the simulation obtained from MLR. The green line is the
243 mean value plus the contribution to the temporal evolution due to chlorine change; the
244 blue line is the mean value plus the contribution due to changes in climate. The fits
245 obtained from the MLR capture the time dependence of each simulation. MLR fitting
246 facilitates comparisons among CCMs by reducing noise due to interannual variability
247 when computing ozone differences for various time periods.
248
249 In all of the CCMs, most of the change in TCO from 1980-2000 is due to chlorine
250 change. For the ensemble of simulations the mean and standard deviation of the ozone
251 decrease between 1980 and 2000 attributed to chlorine increase are -9.4 DU and 4.0 DU.
252 The mean and standard deviation of the ensemble of ozone change due to climate change
253 are 0.8 DU and 0.7 DU, respectively. For the examples in Figure 2 the 60°S-60°N ozone
254 change between 1980 and 2000 due to climate changes is ~1.25 DU. In contrast, the
255 60°S-60°N ozone changes due to chlorine increase are -8.4 DU and -18.4 DU.
256
257 *3.2 Ozone Response in the Upper Stratosphere and Lower Atmosphere*

258 Projected changes in greenhouse gases (GHG) and ODSs will have different impacts on
259 the upper and lower stratospheric ozone because the ozone response to these composition
260 changes varies because the timescales for processes controlling ozone vary with height.
261 In the upper stratosphere, fast radical photochemistry controls the ozone level on
262 timescales of days, while transport controls $O_3$ on seasonal to multi-decadal timescales
263 through the slowly changing levels of long-lived source gases and reservoir species that
264 control the levels of total reactive nitrogen ($NO_y$) and $Cl_y$. In the lower stratosphere
265 where ozone is long-lived, the chemical and transport processes have similar timescales.
266 The predicted speed-up in the Brewer Dobson circulation will affect processes
267 controlling ozone at all timescales through its effects on composition, chemistry,
268 transport, and temperature..
269
270 In addition to its application to the total column ozone as discussed in the previous
271 section, here we use MLR to quantify the effects of GHG and ODS changes on ozone in
272 two partial columns: the upper troposphere and the mid-stratosphere (500 hPa – 20 hPa),
273 hereinafter referred to as the lower atmosphere (LA), and the upper stratosphere (US) (20
274 hPa – 1 hPa). As for the TCO, MLR is applied to timeseries from 1980 to the final
275 simulated year for each CCM. Ozone changes are computed from the resulting MLR fits
276 for time periods when changes in chlorine loading are large (1980-2000) and when they
277 are small (1980-2035). The TCO differences and the contributions from the upper
278 stratosphere and lower atmosphere columns are shown for each CCM in Figure 3. The
279 year 2035 is chosen because it is near the midpoint of the range of return years (2026 –
280 2040) for the CCMs with realistic transport identified by *Strahan et al.* [2011] and also

281 because chlorine change and climate change make similar contributions to the differences
282 in projections as will be discussed in the following section.
283
284 Figure 3a shows that while chlorine loading is increasing (1980-2000), ozone changes are
285 negative in both the LA and US columns in most CCMs. The TCO changes among the
286 CCMs range from -3 to -17 DU; most of this variance comes from the LA response. For
287 the ozone change between 2035 and 1980 (Figure 3b), the LA changes are negative in
288 most CCMs whereas the US changes are positive or less than -0.7 DU. The TCO change
289 can be positive (beyond 'recovery'), near zero ('recovery'), or negative (not yet
290 'recovered'). The range of predicted TCO difference for 2035-1980 (standard deviation
291 2.6 DU) is less than that predicted for 2000-1980 (standard deviation 4.1 DU). The LA
292 changes in this period again contribute the most to the differences among predictions.
293
294 *3.3 Contributions of Chlorine and Climate Change to Ozone Response*
295 *3.3.1 Total Column Ozone Changes*
296 In Figure 4 we separate the chlorine and climate change contributions to the TCO change
297 to explain the variance among CCMs shown in Fig. 3b. Ten CCMs, including the four
298 with the most realistic transport, are clustered near the vertical dashed line, showing the
299 balance between the contributions of chlorine change and climate change among these
300 CCMs that are close to 1980 $O_3$ levels by 2035. Among these CCMs, the TCO change
301 between 1980 and 2035 is most negative for those with the smallest increase due to
302 climate change. Three of the CCMs that are 4 or more DU from their 1980 value are
303 among those with the greatest change due to chlorine; two of these three have negative

304 ozone response due to climate change. The CCM with the earliest recovery (more than
305 2.5 DU greater than 1980 in 2035) has weak sensitivity to chlorine change and the most
306 positive response to climate change.
307
308 *3.3.2 Separation of Processes Affecting Lower and Upper Ozone Columns*
309 From 1980 to 2000, the correlation between upper and lower column ozone responses is
310 0.6; this is not surprising since chlorine related processes dominate the loss in both
311 regions. The correlation gradually declines to 0.2 between 2000 and 2050, as atmospheric
312 chlorine decreases and the contributions from climate change increase. This shows that
313 different mechanisms control the ozone response during different time periods and that
314 upper and lower atmosphere responses of ozone to climate change are not correlated.
315 This prompts separate investigation of the processes contributing to upper and lower
316 column ozone change from 1980.
317
318 *Douglass et al.* [2012] show that upper stratospheric ozone levels prior to 1980 are higher
319 for the CCMs with colder upper atmospheres and vice versa. They use the framework
320 developed by *Stolarski and Douglass* [1985] to explain how differences in unperturbed
321 values for ozone level, temperature and reactive nitrogen contribute to differences in
322 sensitivity of ozone to perturbations in temperature and chlorine. The amplitude of the
323 temperature-dependent annual cycle in ozone varies as expected, decreasing as chlorine
324 increases in all CCMs because the chlorine catalyzed loss cycle is less dependent on
325 temperature. In the LA both photochemical and transport terms are important. Chlorine
326 change has a small impact on the ozone response to temperature change. In this section,

we use MLR to separate the ozone change related to chlorine from other processes in the LA and US, presenting results for two time periods.

Figure 5a shows the simulated ozone changes in the LA from 1980-2000. The response due to chlorine increase (green diamonds) greatly exceeds the ozone change due to climate change (blue triangles) in all but one of the CCMs. In addition, ozone response to increased chlorine contributes much more to inter-model differences than the response to climate change (4.3 DU and 0.6 DU standard deviations, respectively). In comparison, the lower atmosphere ozone difference between 1980 and 2035 due to chlorine is less than half the difference between 1980 and 2000 and there is also less variance among CCMs (Figure 5b). By 2035 middle latitude lower stratospheric inorganic chlorine has decreased by 20-40% from its peak value, depending on the pressure level and CCM being examined, explaining to the smaller contribution from chlorine related processes. The differences among the climate change responses between 2035 and 1980 are larger than those for chlorine.

US changes between 1980 and 2000 (Figure 5c) are broadly similar to the LA but exhibit significantly less model-to-model variability (Figure 5a). The ozone change due to chlorine increase dominates the overall response, and differences in sensitivity to chlorine change contribute to the variability among CCMs. The ozone response to climate change is positive and about 1.1 DU in all CCMs. By 2035 (Figure 5d), the ozone change due to chlorine change has decreased while the $O_3$ increase due to climate change has increased; this increase is both larger and more variable than the ozone decrease due to chlorine.

350 *Douglass et al.* [2012] show that temperature changes are comparable among CCMs, thus
351 the differences in ozone response to climate change reflect differences in ozone
352 sensitivity to temperature. Ozone sensitivity to climate change is similar among CCMs in
353 2000 and different in 2035. This is expected because when ozone loss due to chlorine is
354 a larger fraction of all losses, as in 2000, $O_3$ is less sensitive to temperature change
355 because the chlorine loss reaction is the least temperature dependent of all the loss
356 processes.
357
358 Figure 6 shows how the standard deviation among the 14 simulations of the 60ºS-60ºN
359 TCO differences from 1980 changes between 1980 and 2080, separating the contributions
360 from chlorine change (green) and climate change (blue). Until about 2000, the
361 differences in ozone sensitivity to chlorine change account for nearly all of the variation
362 among CCM predictions. The contribution from climate change rises throughout the
363 integration, equaling the contribution from chlorine change in about 2035. The chlorine
364 contribution to inter-model differences continues to decline as expected as chlorine
365 declines, while the contribution of climate change continues to increase. By 2080, the
366 differences in chlorine sensitivity do not contribute significantly to inter-model
367 differences, and the climate change contribution is ~70% of the magnitude of the peak
368 chlorine contribution in 2005.
369
370 **4. Explaining differences in ozone projections**
371 Figure 1 shows that in 2000 the range of CCM values for the difference from 1980 for
372 60ºS-60ºN or 90ºS-90ºN TCO amounts is approximately 15 DU. By about 2080, the

373 range is about 9 DU and the contribution of the simulated ozone response to stratospheric
374 chlorine change is near zero (Figure 6). The MLR analysis presented in the previous
375 section, summarized by Figure 6, shows that understanding the differences among CCM
376 predictions requires understanding both the differences in ozone sensitivity to chlorine
377 and the differences in ozone sensitivity to climate change, especially in the LA. To
378 explain the narrower range for TCO return to 1980 for CCMs with most realistic
379 transport, we demonstrate the relationship between transport and lower stratosphere
380 distributions of chlorine reservoirs, linking those distributions with the simulated
381 sensitivity of LA ozone to chlorine change.
382
383 All CCMs solve a continuity equation for the ozone mixing ratio $\gamma_{O3}$ at each grid point
384 that includes chemical production (*P),* loss (*L*) and transport terms:

385 $$\frac{\partial \gamma_{O3}}{\partial t} = P - L + transport$$

386 Below about 50 km ozone is very nearly equal to the sum of ozone and atomic oxygen,
387 and photolysis of ozone producing atomic oxygen and reformation of ozone through
388 reaction of atomic and molecular oxygen are in approximate balance. Production is
389 mainly photolysis of molecular oxygen producing two oxygen atoms that form ozone
390 molecules by reaction of atomic and molecular oxygen. In addition to the reaction of
391 atomic oxygen with ozone, catalytic cycles involving hydrogen, nitrogen and chlorine
392 radicals contribute to ozone loss.
393

394 As atmospheric composition changes, realistic computation of the $\partial\gamma_{O3}/\partial t$ requires
395 appropriate contributions from the photochemical and transport terms. A realistic
396 estimate of the fractional change in *L* requires realistic representation of the fractional
397 importance of each catalytic cycle to the total loss in an unperturbed atmosphere. Short-
398 lived radicals (e.g., chlorine monoxide (ClO), hydroxyl (OH) and nitrogen dioxide
399 ($NO_2$)) participate in catalytic ozone loss. Although radicals are short-lived, transport
400 processes affect ozone loss through their influence on the distributions of long-lived
401 gases and reservoir gases Source gases such as chlorofluorcarbons and nitrous oxide
402 ($N_2O$) produce radicals when destroyed in the stratosphere, Reservoir gases such as
403 hydrogen chloride (HCl) and chlorine nitrate ($ClONO_2$) are produced by reactions of
404 radicals with source gases or with each other. *Dessler et al.* [1995] showed that the
405 partitioning between $ClONO_2$ and HCl as observed by instruments on the Upper
406 Atmosphere Research Satellite (UARS) follows expectation; the ratio $ClONO_2$/HCl is
407 quadratically dependent on ozone, linearly dependent on the hydroxyl radical and
408 inversely dependent on methane. In the lower stratosphere the distributions of both
409 ozone and methane are strongly influenced by transport. *Dessler et al.* [1996] showed the
410 broad agreement between observed and expected partitioning of the reservoir $ClONO_2$
411 and the radical chlorine monoxide using UARS observations of ClO, $NO_2$ and $ClONO_2$
412 along with laboratory data. Thus, the influence of transport on radical distributions in the
413 lower stratosphere causes higher levels of $ClONO_2$ to produce higher levels of ClO. Such
414 simulations will have greater contributions of chlorine-catalyzed loss to the ozone
415 tendency.
416

417 Chapter 6 of *CCMVal2010* compared timeseries of HCl and $ClONO_2$ at the Jungfraujoch
418 station (46.6°N) with timeseries simulated by CCMs; these are likely indicators of the
419 simulated lower atmosphere sensitivity to chlorine because for both species more than
420 70% of the total column resides below 20 hPa. The simulated HCl columns shown in
421 Figure 7 span a wide range of values, with peak annual mean values between 3.1 x $10^{15}$
422 and 6.4 x $10^{15}$ molecules/$cm^2$ (disregarding one CCM with an extremely high peak value
423 due to lack of tropospheric rainout of HCl) compared with 4.0 x $10^{15}$, the 1998 – 2001
424 average of HCl column measurements at Jungfraujoch. The simulated columns
425 generally exhibit the observed time dependence because the time dependence of the
426 chlorine containing source gases (e.g., $CFCl_3$ and $CF_2Cl_2$) is controlled by the boundary
427 conditions. The $Cl_y$ produced by destruction of these molecules varies substantially
428 among the CCMs, and differences in $Cl_y$ and its partitioning between the chlorine
429 reservoirs both contribute to the large spread in computed values of the HCl columns.
430
431 The link between transport and gas phase photochemistry in the lower stratosphere is
432 demonstrated by comparisons of observed and simulated HCl columns in Figure 7. We
433 use seven stations that span 68°N-45°S (Table 2) but are outside the polar vortices,
434 avoiding large seasonal variations in their columns [*Santee et al.,* 2008]. The right
435 column compares the subset of CCMs with realistic transport identified by *Strahan et al.*
436 [2011] with observed HCl columns; the left column compares timeseries from the
437 remaining CCMs. For the entire latitude range, observed and simulated HCl columns are
438 in much better agreement for simulations that perform well on transport diagnostics.
439 Because observations are made at irregular intervals throughout the year, the CCM

440 monthly zonal means are compared with daily measurements from each station. Observed
441 variability neither zonally nor monthly averaged, like the CCMs, and so appears much
442 larger.
443
444 We further investigate the partitioning between HCl and $ClONO_2$ reservoirs using
445 observations from the ACE-FTS. Figure 8a shows profiles from the 14 CCMs of
446 $ClONO_2/Cl_y$ ($\approx ClONO_2/(ClONO_2 + HCl$ for 20 hPa and higher pressures in winter) for
447 December 2005. Blue lines indicate the four with most realistic transport, black lines are
448 the others. The red line indicates the December mean of ACE-FTS profiles between
449 40°N-50°N, 50 hPa – 20 hPa; horizontal lines are the standard deviation of the observed
450 profiles. The CCM with the highest values for $ClONO_2/Cl_y$ has a known error in the
451 photochemical mechanism that leads to lower HCl.
452
453 Figure 5 shows that the contribution of chlorine processes to lower atmospheric ozone
454 column change between 2000 and 1980 varies substantially among CCMs. Much of the
455 variation in response is explained by the partitioning of chlorine reservoirs shown in
456 Figure 8b. The sensitivity of lower atmosphere ozone to chlorine change $(\Delta O_3/\Delta Cl_y)$
457 obtained from the MLR is shown as a function of the simulated partitioning of the
458 chlorine reservoirs ($ClONO_2/Cl_y \approx ClONO_2/(ClONO_2+HCl)$ at 45ºN for December 2005
459 in Figure 8b. The symbol color indicates the total chlorine level at 20 hPa, and the range
460 of values from ACE-FTS for December 2005, 40°N-50°N is shown on the color bar. The
461 three CCMs that are least sensitive to chlorine change have lower than observed values of
462 $ClONO_2/Cl_y$, and also higher than observed values for total $Cl_y$. The simulations that are

463 most sensitive to chlorine have higher than observed levels of $ClONO_2/Cl_y$. The
464 sensitivity $\Delta O_3/\Delta Cl_y$ is negatively correlated with $ClONO_2/Cl_y$ between 50 and 10 hPa for
465 all months. The correlation reaches its maximum value between 30 and 20 hPa (the peak
466 for $ClONO_2/Cl_y$) during winter months, and is -0.78 at 20 hPa in December. Note that
467 observations and simulations confirm that for this pressure range distributions of
468 reservoirs control the radical distributions [*Dessler et al.* 1996]. *Stolarski and Douglass*
469 [1986] and *Douglass and Stolarski* [1987] used a one-dimensional model to show larger
470 (smaller) ozone sensitivity to chlorine change for higher (lower) levels of chlorine
471 radicals in the "present" simulated lower atmosphere. The CCMs investigated here
472 produce the same result. Simulations with higher levels of chlorine radicals inferred by
473 partitioning of reservoirs are more sensitive to chlorine change and vice-versa. The
474 transport diagnostics select CCMs with similar $Cl_y$ levels in the lower stratosphere and
475 similar partitioning of reservoirs, implying similar contributions of chlorine catalyzed
476 loss processes to ozone loss. The $Cl_y$ levels and partitioning of reservoirs for the CCMs
477 with most realistic transport also agree with the NDACC columns and the observations
478 from ACE-FTS. This result and the similar TCO increases due to climate change shown
479 in Figure 5 explain narrower range for year-of-return-to-1980 for CCMs with realistic
480 performance on transport diagnostics discussed by *Strahan et al.* [2011].
481
482 As chlorine decreases, the chlorine contribution to the total change in ozone decreases
483 and differences in chlorine reservoir distributions caused by differences in lower
484 stratospheric transport contribute less to the variance in simulated ozone. Figure 6

485 shows that after 2035 the differences in the response to climate change make the larger
486 contribution to the spread among the CCM predictions.
487
488 **5. Stratospheric ozone after 2035**
489 The contributions to ozone change for 2080 – 1980 from chlorine change and from
490 climate change are compared in Figure 9. Although the anthropogenic contribution to $Cl_y$
491 is not zero, the $Cl_y$ level in 2080 is less than the 1980 level, and the annually averaged
492 60ºS to 60ºN total column ozone change relative to 1980 due to chlorine change is always
493 positive, falling between 0.5 and 2.2 DU (Figure 9a). The ozone change due to chlorine
494 change is always positive in the upper stratosphere and is positive in the lower
495 stratosphere with one exception because for all but one CCM the anthropogenic
496 contribution to stratospheric chlorine is smaller in 2080 than in 1980. Chlorine plays a
497 small role compared with climate change, as shown in Figure 9b (note different scales for
498 the y-axis).
499
500 Climate change affects ozone through cooling and through changes in circulation. All
501 CCMs predict a speedup in the Brewer Dobson circulation, leacing to ozone decreases in
502 the tropical lower stratosphere and increases at middle and high latitudes. Stratospheric
503 cooling results in slower rates of ozone loss processes, producing increased ozone.
504 Twelve of the CCMs produce a net ozone increase relative to their 1980 level by 2060 as
505 impact of chlorine change decreases. The maximum predicted increase for 2080 relative
506 to 1980 due to processes related to climate change is more than 8 DU.
507

508 The changes in TCO and the separate contributions from the upper stratosphere and
509 lower atmosphere due to climate related processes are shown in Figure 9b. The standard
510 deviation of the total column ozone increase due to climate change (~3DU) is comparable
511 to the multi-model mean increase (~4DU). This large variance is caused by a bimodal
512 distribution in model differences between the US and LA columns. In the US, the CCMs
513 consistently produce an ozone increase. In the LA, seven of the CCMs predict a
514 contribution of less than 1 DU. For these CCMs the TCO response to climate change is
515 controlled by the US. The mean TCO increase for these seven CCMS is about 5.6 DU,
516 with a standard deviation of 1.2 DU. *Li et al.* [2009] discuss near the cancellation of
517 tropical and extratropical LA ozone changes in the GEOSCCM that leads to a small net
518 LA response to climate change, and show that the TCO increase due to climate change is
519 approximately equal to the increase in the US. In six of the CCMs the LA ozone
520 decrease due to increased tropical upwelling exceeds extratropical increases such that the
521 latitudinally averaged response to climate change is negative. In these six CCMs the LA
522 ozone decrease is opposed by the US increase; mean TCO response is smaller (2.3 DU)
523 but the standard deviation is larger (3.6 DU) compared with the seven CCMs with small
524 contributions from the LA. In one CCM the extratropical increases exceed the tropical
525 decrease; the LA and US increases combine to produce the TCO increase of more than 8
526 DU.
527
528 Although complete information is not available for these fourteen CCMs, this difference
529 in the net lower atmospheric ozone response appears to be linked to differences in the
530 simulated increases in upwelling. For example, Figure 4.11 in *CCMVal2010* shows that

531 the 9 CCMs producing timeseries longer than 100 years fall into two groups. The annual
532 mean upward mass flux at 70 hPa as calculated from w* for a 'high' group containing 5
533 CCMs shows increases from a 1960 value ~5.8 x $10^9$ kg/s to values as high as 7-9.2 x $10^9$
534 kg/s. In contrast, the annual mean upward mass flux at 70 hPa for a 'low' group
535 containing 4 CCMs is initially ~4.8 x $10^9$kg/s and increases to 6-6.5x$10^9$ kg/s. The
536 simulations considered here also included in *CCMVal2010* Figure 4.11 separate into two
537 groups based largely on the change in mass flux. The CCMs in the 'high' group all
538 produce substantial net lower stratospheric ozone decreases due to climate change; the
539 CCMs in the 'low' group all produce more complete cancellation.
540
541 Although the US and LA both contribute to the range of CCM responses; the range of US
542 responses is smaller than that of the LA. *Douglass et al.* [2012] considered the US
543 response in detail, showing that differences in the UA response to temperature change are
544 partially explained by the simulated ozone levels themselves. CCMs that produce higher
545 (lower) ozone levels for the 1960-1980 timeframe are more (less) sensitive to temperature
546 change because the most temperature dependent loss process $O + O_3$ contributes more
547 (less) to the net ozone loss. Although this is not the only factor that affects the simulated
548 response, this approach does give insight into the responses of the outliers. The CCM
549 that produces the largest US ozone response to climate change (> 8 DU) also produces
550 the largest unperturbed US ozone partial column, exceeding the multi-model mean by
551 more than 15%. In contrast, the CCM that produces the smallest upper stratospheric
552 response to climate change (< 3DU) produces an unperturbed US partial ozone column
553 that is about 15% less than the multimodel mean.

554 To summarize, compensation or lack thereof between the LA decrease in tropical ozone
555 and middle and high latitude LA increase contributes much to the range of responses, but
556 whether or not such compensation is produced is not related to performance on transport
557 diagnostics. Figure 1 shows that the CCMs identified with best performance on transport
558 diagnostics separate after about 2050, with predictions of ozone increases for 2 CCMs
559 each at the high and low ends of the range for the 14 CCMs. For the CCMs included in
560 Figure 4.11 of *SPARCCCMVAl,* the high and low predictions of ozone change are
561 consistent with the CCM falling in the group with high change in mass flux (larger LA
562 decrease opposing US increase resulting in smaller TCO increase) and low change in
563 mass flux (more cancellation between tropical and extra-tropical LA ozone changes and
564 larger total column increase).
565
566 The response of the circulation to climate change is robust among the CCMs in the sense
567 that all CCMs predict an increase of tropical upwelling, however the response is less than
568 robust in two ways. First, the rate of increase varies, and in some of the CCMs the
569 appearance and disappearance of the ozone hole affects the rate of increase. For
570 example, *Li et al.* [2009] show that in the GEOSCCM the rate of increase is about 1/3
571 faster during the formation phase of the ozone hole and 1/3 slower as the ozone hole
572 dissipates compared with the rate of increase in the late 2000's when chlorine change
573 ceases to be significant. Note that GEOSCCM is in the group with 'low' change in
574 annual mean upward mass flux at 70 hPa. Analysis of the time dependence of the annual
575 mean upwelling for the subset of CCMs that provide timeseries of w* shows that the rate
576 of increase may be faster, slower or unaffected by ozone hole formation and dissipation.

577 Second, the extratropical circulation changes and their convolution with simulated lower
578 stratospheric ozone vary substantially. There are differences in both the tropical decrease
579 and in the extratropical increase that result in near cancellation or lack thereof. Both of
580 these factors contribute to the differences among CCM predictions for 21st century ozone.
581
582 **6. Conclusions**
583 This work quantifies the ozone response to changes in chlorine containing source gases
584 and changing climate (i.e., stratospheric cooling and circulation change) in 14 CCMs that
585 participated in CCMVal and contributed simulations to *WMO2010*. All models used the
586 same time-dependent mixing ratio boundary conditions for source gases from 1960-2100.
587 In 2035, ozone decreases relative to 1980 due to chlorine in all CCMs, since chlorine is
588 still substantially elevated compared with 1980. The response to climate change is
589 generally but not always positive. The 60ºS-60ºN annual mean ozone is within 2 DU of
590 1980 levels (i.e., $\Delta TCO < 1\%$) for ten of the CCMs by 2035.
591
592 *Strahan et al.* [2011] showed a narrower range of recovery dates for the CCMs with best
593 performance on the CCMVal transport diagnostics compared with the range for the entire
594 group. This work shows that differences in the sensitivity to chlorine change make the
595 larger contribution to the spread in years for return-to-1980. These differences in
596 chlorine sensitivity are explained by differences in the middle latitude lower stratospheric
597 columns of chlorine reservoirs and differences in partitioning between HCl and $ClONO_2$.
598 The transport diagnostics narrow the range of responses because they select CCMs with a
599 much narrower and more realistic range of column values and partitioning among

chlorine reservoirs than produced by the suite of CCMs. By 2035 12 of 14 CCMs show an ozone increase due to climate change that is between 1 and 4 DU. The CCMs with latest recovery are either more sensitive to chlorine change or less sensitive to climate change than the CCMs identified as having most realistic transport. The CCM with much earlier recovery is least sensitive to chlorine change and among the most sensitive to climate change.

We emphasize the value of the comparisons with NDACC column measurements of the chlorine reservoirs along with comparisons of partitioning among chlorine reservoirs obtained from ACE $ClONO_2$ and HCl profiles, as these comparisons provide a mechanism to explain the variation in the sensitivity to chlorine change by linking lower stratospheric transport with chemistry through the control of the distributions of chlorine reservoir species. CCMs that are most sensitive to chlorine have higher values for $ClONO_2/Cl_y$. The column amounts of HCl and $ClONO_2$ depend both on total $Cl_y$ in the lower atmosphere and its partitioning between the chlorine reservoirs. Because of the mixing ratio boundary conditions, stratospheric $Cl_y$ can vary widely depending on the simulated transport. However, even CCMs with the most lower-atmospheric chlorine need not be the most sensitive to chlorine change, if they partition chlorine reservoirs towards HCl at the expense of $ClONO_2$. The ozone response to chlorine change depends on reactions with short-lived radical species; their levels are controlled by both the total $Cl_y$ and its partitioning between the reservoir species HCl and $ClONO_2$.

623 In 2035, the simulated response to climate change is similar for the CCMs with most
624 realistic transport; for 12 of the 14 CCMs the response to climate change is positive and
625 between 1 and 4.5 DU. As the simulations continue, differences in the ozone response to
626 changes in circulation and temperature grow. In the US the 60ºS-60ºN annual average
627 ozone increases in all CCMs, and the differences in the magnitude of the increase are
628 explained by differences in the importance of the various catalytic loss cycles, such that
629 simulations with highest ozone in the unperturbed (low chlorine) period (~1960 – ~1980)
630 are most sensitive to temperature change [*Douglass et al*., 2012]. These differences
631 account for about one third of the spread in predictions. The LA ozone response is more
632 complicated, as both circulation change and temperature change contribute. Although the
633 CCMs all predict increased upwelling, the rate of increase varies among CCMs. *Li et al*.
634 [2009] show a much larger rate of increase in w* during ozone hole formation than
635 during ozone hole dissipation for GEOSCCM. There is no consensus among CCMs as to
636 the impact of the ozone hole on the rate of increase of w*. *Li et al*. [2009] also note LA
637 cancellation of the impacts of the speedup of the Brewer Dobson Circulation between
638 tropical and extratropical latitudes, i.e., the tropical ozone decrease that accompanies
639 upwelling increase is opposed by middle and high latitude ozone increase. Seven of the
640 14 CCMs (including GEOSCCM) behave in a similar manner, and the net LA change due
641 to climate change for this subgroup is less than 1 DU for 2080 relative to 1980. For six
642 of the CCMs the LA impact due to climate change is substantially negative, and for one
643 the net LA impact due to climate change is substantially positive. These differences
644 contribute most to the differences in projections in the late 21$^{st}$ century. The CCMVal
645 diagnostics do not discriminate among the projections for w* or the cancellation between

646 tropical and extratropical response. Reduction of the spread among predictions for future
647 ozone levels requires further investigation in the differences in the response of the
648 Brewer Dobson Circulation to increasing GHGs.
649
650 This analysis shows that the differences in projections for ozone can be explained. The
651 US responses would be similar if the catalytic loss cycles were represented in the same
652 balance; therefore it is important to use observations to assure that the loss cycles are
653 represented in the appropriate balance in order to identify the 'best' prediction [e.g.,
654 *Douglass et al*., 2011]. Similarly, the near linear dependence of the ozone sensitivity to
655 chlorine on the partitioning between $ClONO_2$ and HCl suggest that LA responses to
656 chlorine change will be similar if the reservoir distributions are similar, therefore it is
657 important to use observations such as NDACC columns and profiles from ACE-FTS to
658 assure that the reservoir distributions are realistic. In this case, deficiencies in transport
659 relate directly to differences in the simulated response to composition change. The lower
660 stratospheric ozone evolution is simple to diagnose given the evolution of w*. Although
661 it is not possible at this time to explain differences among simulations for w*, it is likely
662 that, as data records lengthen, analysis of observations in the tropics will make provide
663 limits for the rate of change of w* using such quantities as the lower stratospheric ozone
664 or the amplitude of the quasi-biennial oscillation [*Randel and Thompson*, 2011; *Kawatani*
665 *and Hamilton*, 2013].
666
667 Finally, these results, in particular linking transport diagnostics, unrealistic reservoir
668 distributions and differences in sensitivity of simulated lower atmospheric ozone to

669 chlorine change, question the value of the use of a multi-model mean as a best prediction
670 of 21st century ozone. Differences in simulated responses that can be traced to biases and
671 understood are clearly not random. This study has identified the causes for differences in
672 CCM ozone projections and explained the differences in lower atmosphere sensitivity to
673 chlorine change. This work demonstrates that diagnostics used to evaluate CCM
674 performance are most useful when they are linked with a mechanism that is related to a
675 model's response to a perturbation. The use of such diagnostics supports a strategy to
676 reduce uncertainty in prediction.
677
678 *Acknowledgements*
679 We acknowledge the modeling groups for making their simulations available for this
680 analysis. The Chemistry-Climate Model Validation Activity (CCMVal) for WCRP's
681 (World Climate research Programme) SPARC (Stratospheric Processes and their Role in
682 Climate) project for organizing and coordinating the model data analysis activity, and the
683 British Atmospheric Data Center (BADC) for collecting and archiving the CCMVal
684 model output.
685
686 The data used in this publication were obtained as part of the Network for the Detection
687 of Atmospheric Composition Change (NDACC) and are publicly available (see
688 http://www.ndacc.org).
689
690
691

692

693

694

694 REFERENCES

695 Akiyoshi, H., L. B. Zhou, Y. Yamashita, K. Sakamoto, M. Yoshiki, T. Nagashima, M.
696 Takahashi, J. Kurokawa, M. Takigawa, and T. Imamura (2009), A CCM
697 simulation of the breakup of the Antarctic polar vortex in the years 1980–2004
698 under the CCMVal scenarios, *J. Geophys. Res., 114*, D03103,
699 doi:10.1029/2007JD009261.

700 Austin, J., and R. J. Wilson (2006), Ensemble simulations of the decline and recovery of
701 stratospheric ozone, *J. Geophys. Res., 111*, D16314, doi:10.1029/2005JD006907.

702 Bekki, S. and G. E. Bodeker (Coordinating Lead Authors) et al. (2011), Future ozone and
703 its impact on surface UV, Chapter 3 in *Scientific Assessment of Ozone Depletion:*
704 *2010,* Global Ozone Research and Monitoring Project – Report No. 52, 516 pp.,
705 World Meteorological Organization, Geneva, Switzerland.

706 Bernath, P. F., et al. (2005), Atmospheric Chemistry Experiment (ACE): Mission
707 overview, Geophys. Res. Lett., 32, L15S01, doi:10.1029/ 2005GL022386.

708 Butchart N., et al. (2006), Simulations of anthropogenic change in the strength of the
709 Brewer–Dobson circulation, *Clim. Dyn. 27,* 727–741.

710 Butchart, N., et al. (2010), Chemistry–Climate Model Simulations of Twenty-First
711 Century Stratospheric Climate and Circulation Changes, *J. Clim., 23,* 5349-5373.

712 Davies, T., M. J. P. Cullen, A. J. Malcolm, M. H. Mawson, A. Staniforth, A. A. White,
713 and N. Wood (2005), A new dynamical core for the Met Office's global and
714 regional modelling of the atmosphere, *Q. J. R. Meteorol. Soc., 131*, 1759–1782,
715 doi:10.1256/qj.04.101.

716 Déqué, M. (2007), Frequency of precipitation and temperature extremes over France in
717 an anthropogenic scenario: Model results and statistical correction according to
718 observed values, *Global Planet. Change, 57*, 16–26,
719 doi:10.1016/j.gloplacha.2006.11.030.
720 de Grandpré, J., S. R. Beagley, V. I. Fomichev, E. Griffioen, J. C.McConnell, A. S.
721 Medvedev, and T. G. Shepherd (2000), Ozone climatology using interactive
722 chemistry: Results from the Canadian Middle Atmosphere Model, *J. Geophys.*
723 *Res., 105,* 26,475–26,491, doi:10.1029/ 2000JD900427.
724 Dessler, A. E., et al. (1995), Correlated observations of HCl and $ClONO_2$ fro UARS and
725 implications for stratospheric chlorine partitioning, *Geophys. Res. Lett., 22*, 1721-
726 1724.
727 Dessler, A. E., R. Kawa, A. Douglass, D. Considine, J. Kumer, J. Waters, J. Gille (1996),
728 A Test of the Partitioning Between ClO and $ClONO_2$ Based on Simultaneous
729 UARS Measurements of ClO, $NO_2$, and $ClONO_2$, *J. Geophys. Res., 101*, 12,515-
730 12,521.
731 Douglass, A. R., and R. S. Stolarski, The use of atmospheric measurements to constrain
732 model predictions of ozone change from chlorine perturbations, *J. Geophys. Res.,*
733 *92,* 6662-6674, 1987.
734 Douglass, A. R. and V. Fioletov (Coordinating Lead Authors), S. Godin-Beekman, R.
735 Müller, R. S. Stolarski, and A. Webb (2011), Stratospheric Ozone and Surface
736 Ultraviolet Radiation, Chapter 2 in *Scientific Assessment of Ozone Depletion:*
737 *2010,* Global Ozone Research and Monitoring Project Report No. 52, World
738 Meteorological Organization, Geneva, Switzerland.

739 Douglass, A. R., R. S. Stolarski, S. E. Strahan, and L. D. Oman (2012), Understanding
740 differences in upper stratospheric ozone response to changes in chlorine and
741 temperature as computed using CCMVal-2 models, *J. Geophys. Res., 117*,
742 D16306, doi:10.1029/2012JD017483
743 Eyring, V., et al. (2005), A strategy for process-roiented validation of coupled chemistry-
744 climate models, *Bull. Am. Meteorol. Soc., 86,* 1117-1133.
745 Garcia, R. R., D. Marsh, D. E. Kinnison, B. Boville, and F. Sassi (2007), Simulations of
746 secular trends in the middle atmosphere, 1950–2003, *J. Geophys. Res., 112*,
747 D09301, doi:10.1029/2006JD007485.
748 IPCC (Intergovernmental Panel on Climate Change) (2000), *Special Report on Emissions*
749 *Scenarios: A Special Report of Working Group III of the Intergovernmental Panel*
750 *on Climate Change,* 599 pp., Cambridge Univ. Press, Cambridge, U. K.
751 Jourdain, L., S. Bekki, F. Lott and F. Lefevre (2008), The coupled chemistry-climate
752 model LMDZ-REPROBUS: Description and evaluation of a transient simulation
753 of the period 1980 – 1999, *Ann. Geophys., 26,* 1391-1413, doi:10.5194/angeo-26-
754 1391-2008.
755 Kawatani, Y., and K. Hamilton (2013), Weakened stratospheric quasibiennial oscillation
756 driven by increased tropical mean upwelling, *Nature, 497,* 478-
757 482,doi:10.1038/nature12140.
758 Li., F., R. S. Stolarski and P. A. Newman (2009), Stratospheric ozone in the post-CFC
759 era, *Atmos. Chem. Phys., 9,* 2207–2213, doi:10.5194/acp-9-2207-2009.
760 Morgenstern, O., P. Braesicke, F. M. O'Connor, A. C. Bushell, C. E. Johnson, S. M.
761 Osprey, and J. A. Pyle (2009), Evaluation of the new UKCA climate composition

762 model. Part 1: The stratosphere, *Geosci. Model Dev., 2*, 43–57, doi:10.5194/gmd-
763 2-43-2009.
764 Morgenstern, O., et al. (2010), Review of the formulation of present generation
765 stratospheric chemistry-climate models and associated external forcings, *J.*
766 *Geophys. Res., 115,* D00M02, doi:10.1029/2009JD013728.
767 Newman, P. A., J. Daniel, D. Waugh, and E. Nash (2007), A new formulation of
768 equivalent effective stratospheric chlorine (EESC), *Atmos. Chem. Phys.*, *7*, 4537–
769 4552.
770 Oman, L. D., et al. (2010), Multimodel assessment of the factors driving stratospheric
771 ozone evolution over the 21st century, J. *Geophys. Res., 115*, D24306,
772 doi:10.1029/2010JD014362.
773 Pawson, S., R. S. Stolarski, A. R. Douglass, P. A. Newman, J. E. Nielsen, S. M. Frith,
774 and M. L. Gupta (2008), Goddard Earth Observing System chemistry-climate
775 model simulations of stratospheric ozone-temperature between 1950 and 2005, *J.*
776 *Geophys. Res., 113,* D12103, doi:101029/2007JD009511.
777 Pitari, G., E. Mancini, V. Rizi, and D. T. Shindell (2002), Impact of future climate and
778 emission changes on stratospheric aerosols and ozone, *J. Atmos. Sci., 59*, 414–
779 440, doi:10.1175/1520-0469.
780 Randel, W. J., and A. M. Thompson (2011), Interannual variability and trends in tropical
781 ozone derived from SAGE II satellite data and SHADOZ ozonesondes, *J.*
782 *Geophys. Res., 116*, D07303, doi:10.1029/2010JD015195.

783 Rinsland, C. P., et al. (2003) Long-term trends of inorganic chlorine from ground-based
784 infrared solar spectra: Past increases and evidence for stabilization, *J. Geophys.*
785 *Res., 108*, doi:10.1029/2002JD003001.
786 Santee, M. L., I. A. MacKenzie, G. L. Manney, M. P. Chipperfield, P. F. Bernath, K. A.
787 Walker, C. D. Boone, L. Froidevaux, N. J. Livesey, and J. W. Waters (2008), A
788 study of stratospheric chlorine partitioning based on new satellite measurements
789 and modeling, *J. Geophys. Res., 113*, D12307, doi:10.1029/2007JD009057.
790 Schraner, M., et al. (2008), Technical Note: Chemistry-climate model SOCOL: Version
791 2.0 with improved transport and chemistry/microphysics schemes, *Atmos. Chem.*
792 *Phys., 8*, 5957–5974, doi:10.5194/acp-8-5957-2008.
793 Scinocca, J. F., N. A. McFarlane, M. Lazare, J. Li, and D. Plummer (2008), Technical
794 note: The CCCma third generation AGCM and its extension into the middle
795 atmosphere, *Atmos. Chem. Phys., 8*, 7055–7074, doi:10.5194/acp-8-7055-2008.
796 Scinocca, J.F., D.B. Stephenson, T.C. Bailey, and J. Austin (2010), Estimates of past and
797 future ozone trends from multi-model simulations using a flexible smoothing
798 spline methodology, *J. Geophys. Res*., *115,* D00M12,
799 doi:10.1029/2009/JD013622.
800 Shepherd, T. G. (2008), Dynamics, stratospheric ozone, and climate change, *Atmos.*
801 *Ocean, 46*, 117–138, doi:10.3137/ao.460106.
802 Shibata, K., and M. Deushi (2008a), Long-term variations and trends in the simulation of
803 the middle atmosphere 1980–2004 by the chemistry climate model of the
804 Meteorological Research Institute, *Ann. Geophys., 26*, 1299–1326,
805 doi:10.5194/angeo-26-1299-2008.

Shibata, K., and M. Deushi (2008b), Simulation of the stratospheric circulation and ozone during the recent past (1980 – 2004) with the MRI chemistry-climate model, CGER's Supercomp. Monogr. Rep., 14, 154pp., Cent for Gobal Environ. Res., Natl. Inst. For Environ. Studies, Tsukuba, Japan.

SPARC CCMVal (2010), SPARC Report on the Evaluation of Chemistry-Cliamte Models, V. Eyring, T. G. Shepherd, D. W. Waugh (Eds.), SPARC Report No. 5, WcRP-32, WMO/TD-No. 1526.

Stolarski, R. S., and A. R. Douglass (1985), Parameterization of the photochemistry of stratospheric ozone including catalytic loss processes, *J. Geophys. Res., 90,* 10,709-10,718.

Stolarski, R. S., and A. R. Douglass (1986), Sensitivity of an atmospheric photochemistry model to chlorine perturbations including consideration of uncertainty propagation, *J. Geophys. Res, 91,* 7853-7864.

Stolarski, R. S., P. Bloomfield, R. D. McPeters and J. R. Herman (1991), Total Ozone Trends Deduced From Nimbus 7 Toms Data, *Geophys. Res., Lett., 6,* 1015-1018.

Stolarski, R. S., A. R. Douglass, S. Steenrod, S. Pawson (2006), Trends in stratospheric ozone: lessons learned from a 3D chemical transport model, *J. Atmos. Sci., 63*, 1028-1041.

Stolarski, R. S., A. R. Douglass, P. A. Newman, S. Pawson, M. R. Schoeberl (2009), Relative Contribution of Greenhouse Gases and Ozone-Depleting Substances to Temperature Trends in the Stratosphere: A Chemistry–Climate Model Study, *J. Clim., 23,* 28-41.

829 Strahan, S. E., et al. (2011), Using transport diagnostics to understand chemistry climate
830 model ozone simulations, *J. Geophys. Res., 116*, D17302,
831 doi:10.1029/2010JD015360.
832 Teyssèdre, H., et al. (2007), A new tropospheric and stratospheric chemistry and
833 transport model MOCAGE-Climat for multi-year studies: Evaluation of the
834 present-day climatology and sensitivity to surface processes, *Atmos. Chem. Phys.,*
835 *7*, 5815–5860, doi:10.5194/acp-7-5815-2007.
836 Tian, W., and M. P. Chipperfield (2005), A new coupled chemistry-climate of the
837 stratosphere: The importance of coupling for future O3-climate predictions, *Q. J.*
838 *R. Meteorol. Soc., 131,* 281-303, doi:10.1256/qj.04.05.
839 Tian, W., M. P. Chipperfield, L. J. Gray, and J. M. Zawodny (2006), Quasibiennial
840 oscillation and tracer distributions in a coupled chemistry-climate model, *J.*
841 *Geophys. Res., 111,* D20301, doi:10.1029/2005JD006871.
842 Waugh, D. W., and V. Eyring (2008), Quantitative performance metrics for stratospheric-
843 resolving chemistry-climate models, *Atmos. Chem. Phys., 8*, 5699-5713.
844 Waugh, D. W., Oman, L., Kawa, S. R., Stolarski, R. S., Pawson S., Douglass, A. R.,
845 Newman, P. A., and Nielsen, J. E. (2009), Impacts of climate change on
846 stratospheric ozone recovery, *Geophys. Res. Lett., 36*, L03805,
847 doi:10.1029/2008GL036223.
848 WMO (World Meteorological Organization) (2007), *Scientific assessment of ozone*
849 *depletion: 2006*, Global Ozone Research and Monitoring Project – Report No.
850 50, 572 pp., Geneva, Switzerland.
851

WMO (World Meteorological Organization) (2011), *Scientific Assessment of Ozone Depletion: 2010:* Global Ozone Research and Monitoring Project – Report No. 52, 516 pp., Geneva, Switzerland.

858 Table 1

| Model | Reference |
|---|---|
| **AMTRAC3** | *Austin and Wilson* [2010] |
| **CCSRNIES** | *Akiyoshi et al*. [2009] |
| **CMAM** | *Scinocca et al*. [2008]; *de Grandpré et al*. [2000] |
| **CNRM-ACM** | D*équé* [2007]; *Teyssièdre et al.* [2007] |
| **GEOSCCM** | *Pawson et al.* [2008] |
| **LMDZrepro** | *Jourdain et al.* [2008] |
| **MRI** | *Shibata and Deushi [2008a; 2008b]* |
| **Niwa-SOCOL** | *Schraner et al.* [2008] |
| **SOCOL** | *Schraner et al.* [2008] |
| **ULAQ** | *Pitari et al.* [2002] |
| **UMSLIMCAT** | *Tian and Chipperfield* [2005]; *Tian et al.* [2006] |
| **UMUKCA-METO** | *Davies et al.* [2005]; *Morgenstern et al.* [2009] |
| **UMUKCA-UCAM** | *Davies et al.* [2005]; *Morgenstern et al.* [2009] |
| **WACCM** | *Garcia et al.* [2007] |

859

860

860 Table 2

| Station | Location |
|---|---|
| Kiruna, Sweden | 67.84°N 20.41° E |
| Harestua, Norway | 60.2°N 10.8 °E |
| Jungfraujoch, Switzerland | 46.55°N 7.98 °E |
| Kitt Peak, AZ, USA | 31.9°N 111.6°W |
| Izaña (Tenerife), Spain | 28.30°N 16.48°W |
| Mauna Loa, HI, USA | 19.54°N 155.58°W |
| Lauder, New Zealand | 45.04°S 169.68°E |

861

861 FIGURES

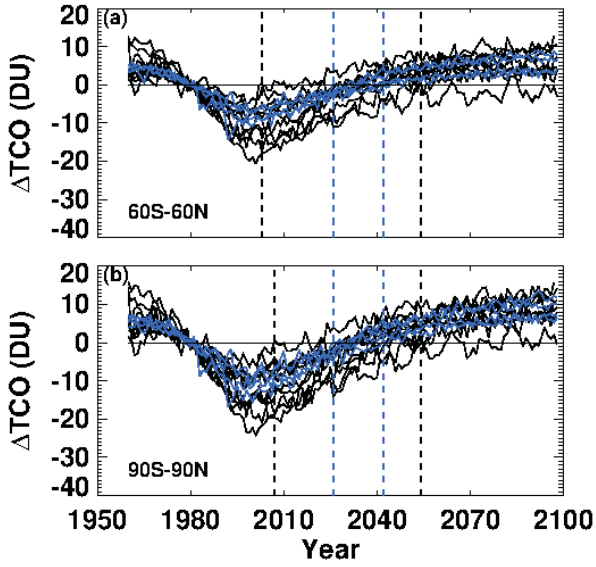


862

863

864 **Figure 1** a) The difference in the TCO from the 1978-1982 mean for 60°S-60° as

865 simulated by CCMVal models; b) same as a) for 90°S-90°N. In both panels the blue

866 traces identify CCMs with most realistic transport. The dashed black vertical lines

867 indicate the range of years for return to 1980 for the entire group of CCMs; the blue

868 vertical lines indicate the narrower range for the CCMs with most realistic transport.

869

870

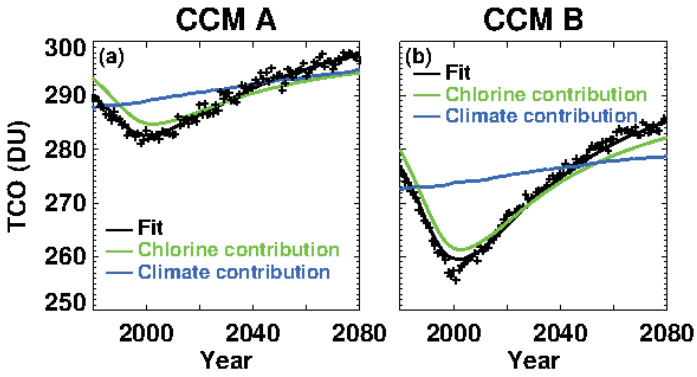


**Figure 2** 60°S-60°N average column ozone from two of the CCMVal CCMs. The crosses are the annually averaged columns; the black, green and blue lines are the fit obtained using the MLR, the contribution due to chlorine change and the contribution due to climate change respectively. The ozone response to climate change is similar for these examples, but the ozone response to chlorine change differs by more than a factor of 2.

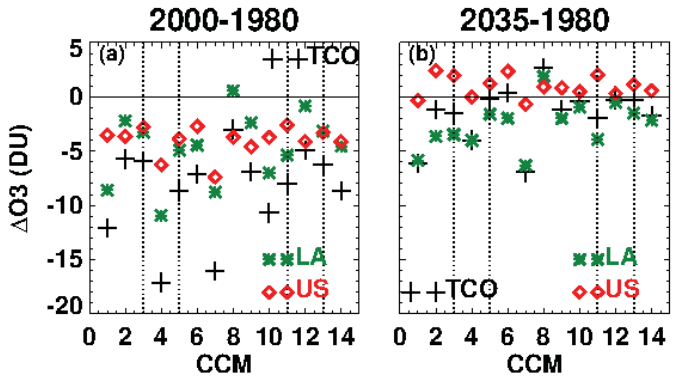


**Figure 3** The upper stratosphere and lower atmosphere contributions to the 60ºS-60ºN change in TCO between 1980 and 2000 (left) and 1980 and 2035 (right). For both time intervals, the LA contributes more to the differences in CCM predictions than US. The dotted vertical lines identify the CCMs with most realistic transport.

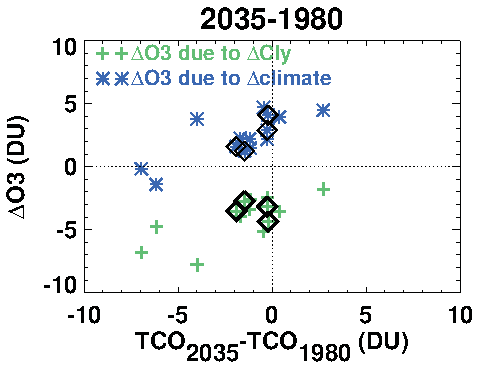


884

885 **Figure 4** The 2035 – 1980 60ºS-60ºN contribution due to chlorine change (crosses, y-
886 axis) and that due to climate change (stars, y-axis) as functions of the change in TCO (x-
887 axis). The black symbols indicate the CCMs with most realistic transport.

888

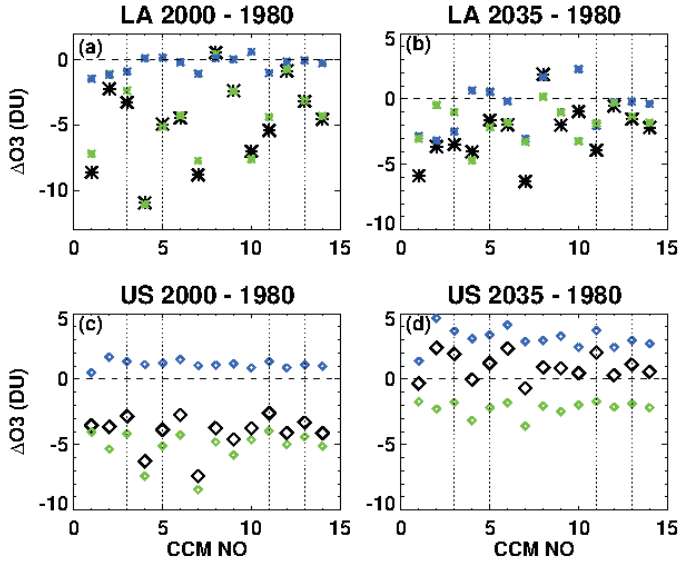


889

890 **Figure 5** a) The 60°S-60°N LA ozone column change between 2000 and 1980 (crosses),
891 the contribution due to chlorine change (green diamonds), and the contribution due to
892 climate change (blue triangles); b) Same as a) for 2035 and 1980; c) same as a) for the
893 US; d) same as b) for the US. The dotted vertical lines identify the CCMs with most
894 realistic transport.

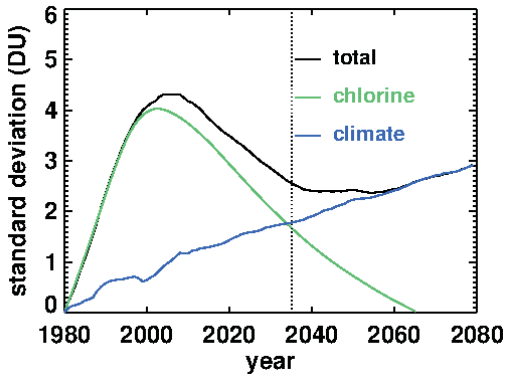


**Figure 6** CCM variance for each year between 1980-2080 of the difference from 1980 TCO. The MLR results are used to produce separate time series for the contribution due to chlorine change and the contribution due to climate change. The standard deviations are shown here for the total difference (black), the chlorine contribution (green) and the contribution due to climate change.

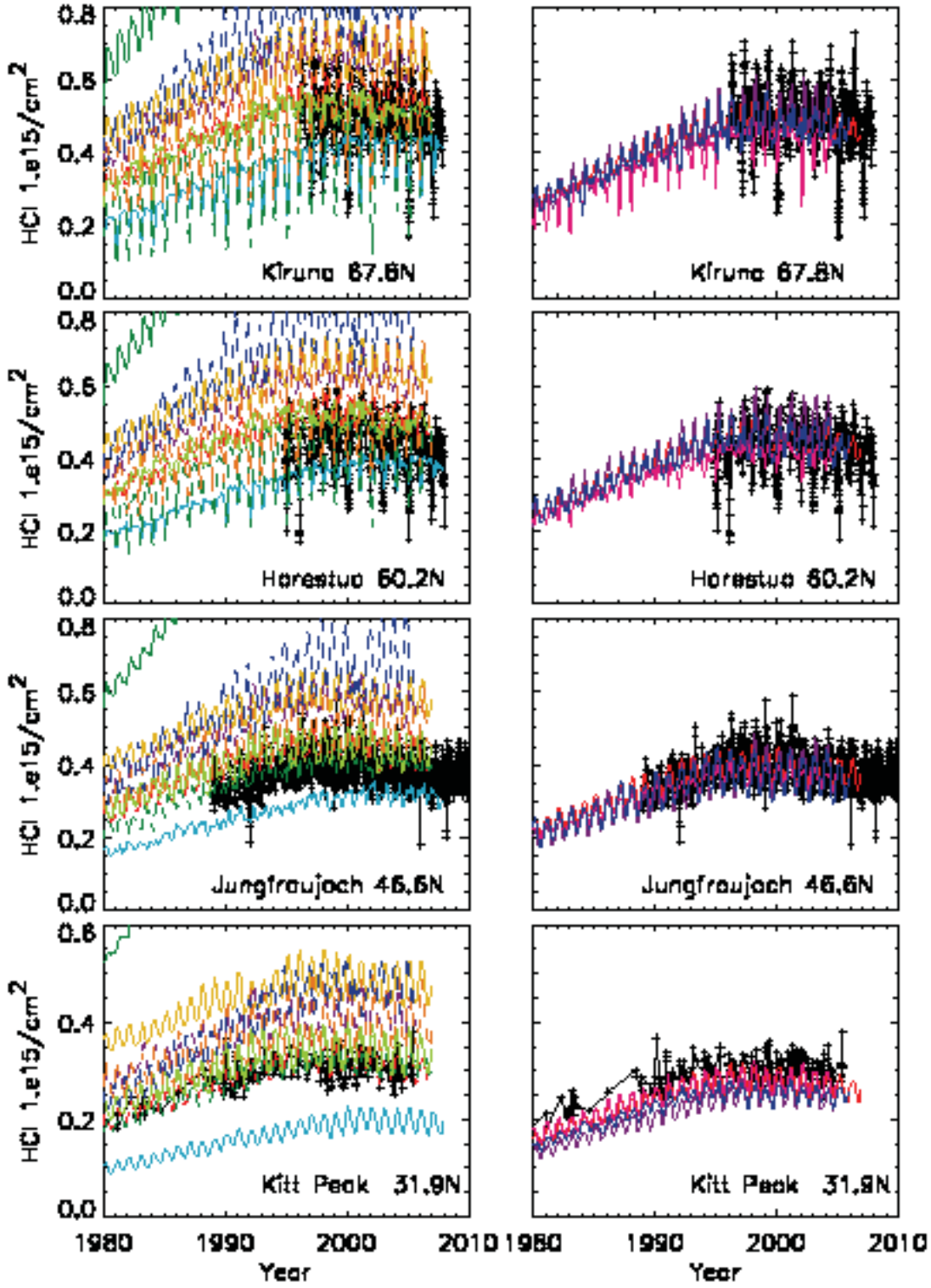
HCl 1.e15/cm$^2$
Kiruna 67.8N
Harestua 60.2N
Jungfraujoch 46.6N
Kitt Peak 31.9N
0.0
0.2
0.4
0.6
0.8
1980
1990
2000
2010
Year

902

903

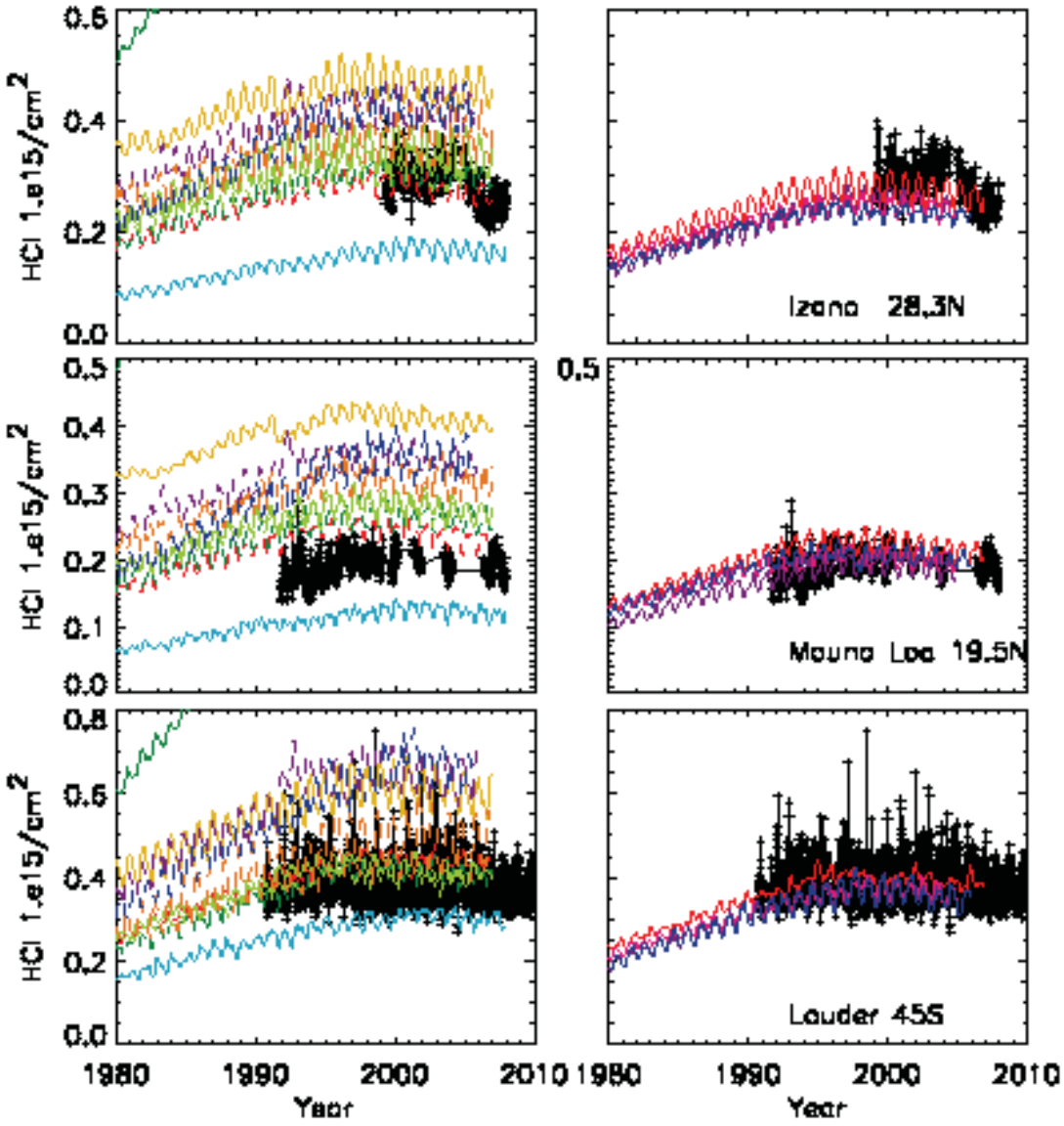


904

905 **Figure 7** Monthly zonal mean simulated HCl columns at 7 NDACC stations spanning a latitude

906 range 67.8°N – 45°S for CCMs with most realistic transport (right column) and for the remaining

907 CCMs (left column). Measurements are overhead columns (molecules/cm$^2$).

908

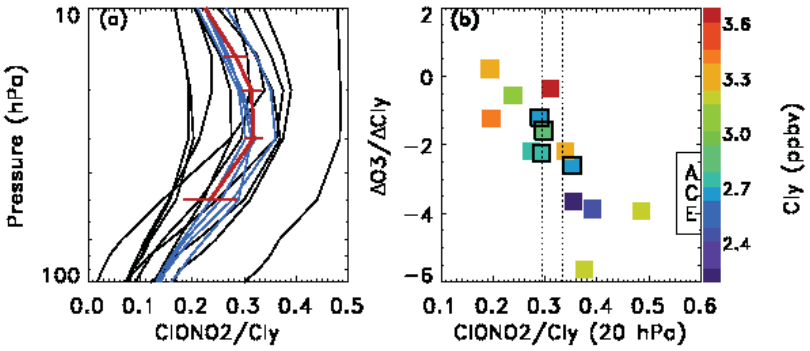


909

910 **Figure 8** a) The December 2004 mean $ClONO_2/Cl_y$ for 45°N from the ACE

911 measurements (red solid line), from the 4 CCMs with most realistic transport (blue solid

912 lines), and from the rest of the CCMs (black solid lines). Horizontal bars on the ACE

913 profile indicate the standard deviation. b) The sensitivity of lower atmosphere ozone to

914 chlorine change ($\Delta O_3/\Delta Cl_y$) obtained from the MLR as a function of the simulated ratio

915 $ClONO_2/Cl_y$ at 20 hPa. The CCMs with most realistic transport are outlined by black

916 squares. Vertical dashed lines indicate the ACE estimate for $ClONO_2/Cl_y$ at 20 hPa. The

917 colors of the symbols correspond to the total $Cl_y$ at 20 hPa – the ACE estimate is

918 indicated on the color bar. The correlation coefficient between ClONO$_2$/Cly and

919 $\Delta O_3/\Delta Cl_y$ is -0.78.

920

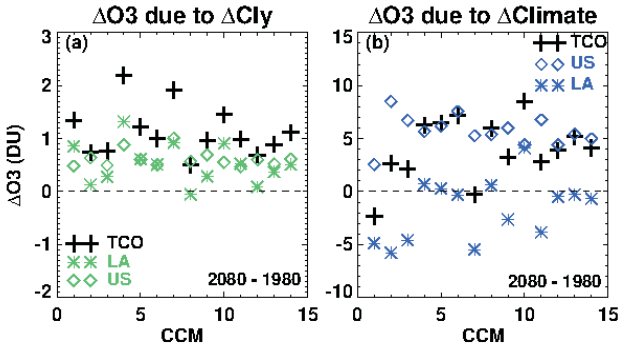


**Figure 9** a) ozone change due to chlorine change, 2080 – 1980, upper stratosphere and lower atmosphere; b) ozone change due to climate change, 2080 – 1980, upper stratosphere and lower atmosphere.